



Cite this: *Analyst*, 2018, **143**, 2908

An enzymatic polymerization-activated silver nanocluster probe for *in situ* apoptosis assay†

Rong Zhu, Xingyu Luo, Lu Deng, Chunyang Lei,  * Yan Huang,  Zhou Nie* and Shouzhuo Yao

As an emerging category of fluorophores, nucleic acid-stabilized silver nanoclusters (DNA/AgNCs) have attracted a great deal of interest and have been widely applied for interdisciplinary research. In this work, we have constructed a novel DNA/AgNC probe for cell apoptosis detection and imaging based on an enzyme-polymerized polyadenylic acid (poly-dA) DNA chain and a toehold strand displacement reaction. This method can effectively “tag” intracellular genomic DNA fragments, a biochemical hallmark of apoptosis, with poly-dA DNA chains up to 400-bases produced by terminal deoxynucleotidyl transferase (TdT)-activated polymerization. The strand displacement initiated by the target poly-dA DNA chain releases the quencher labeled-DNA from the DNA/AgNC probe, leading to a significant fluorescence lighting-up of DNA/AgNCs for the sensitive detection of cell apoptosis, with a high signal-to-background ratio (S/B = 58). Using the DNA/AgNC-based assay, as few as 20 apoptotic cells can be detected *in vitro*. Furthermore, the feasibility of our approach was demonstrated by the *in situ* quantitative analysis of apoptosis in HepG2 cells without the need for tedious washing and separation steps.

Received 22nd March 2018,
Accepted 4th May 2018

DOI: 10.1039/c8an00535d

rscl.li/analyst

Introduction

Apoptosis, a highly regulated process of programmed cell death, plays an essential role in the regulation of cell balance and maintaining tissue homeostasis.^{1,2} Abnormal regulation of the cell apoptosis can ultimately lead to a wide variety of diseases, such as myocardial infarction, neurodegenerative disorders, autoimmune disorders, atherosclerosis and cancers.^{3,4} The detection and monitoring of cell apoptosis has great implications for advancing apoptotic investigations and evaluating the efficacy of apoptosis-targeted antitumor therapies.^{5–8} Several characteristic biochemical changes occur, including phosphatidylserine (PS) exposure to the extracellular leaflet of the plasma membrane, protease activation and DNA fragmentation when cells are subjected to apoptosis.^{9,10} And numerous strategies have been developed to monitor the apoptosis progress according to the various biochemical characteristics of apoptotic cells. For example, Annexin V assay based on the high affinity between exposed PS and Annexin V protein,¹¹ can quantify the number of cells undergoing apoptosis, while the false positive results from necrotic cells cannot be avoided.¹²

DNA ladder assay could evaluate cell apoptosis by monitoring the characteristic DNA fragments by gel electrophoresis, but with the drawbacks of low sensitivity, non-quantitative analysis, and labor-intensive and time-consuming procedures.¹³ To overcome these limitations, terminal deoxynucleotidyl transferase (TdT)-mediated dUTP nick-end labeling (TUNEL assay) was introduced for an *in situ* study of apoptosis based on the TdT-mediated incorporation of labeled dUTP to the 3'-OH ends of DNA double strand breaks (DSBs).¹⁴ Although TUNEL assay is efficient for *in situ* probing cell apoptosis, its usage is still hampered by the relatively high cost of labeled nucleotides and multiple separation and washing steps.^{15,16} To address these issues, developing a “switch-on” probe with a low background would provide an alternative for designing improved strategies for cell apoptosis probing.

To date, noble metal nanoclusters composed of several to tens of metal atoms with a typical size of less than 2 nm, have emerged as a kind of novel material attracting much attention.^{17,18} Due to their ultra-small sizes that are comparable to the Fermi wavelength of electrons, noble metal nanoclusters exhibit some unique properties, including discrete electronic transitions and strong fluorescence emission.^{19,20} Extensive efforts have been devoted to the facile synthesis of fluorescent and well-dispersed metal nanoclusters utilizing biocompatible scaffolds, such as peptides,²¹ proteins^{22,23} and nucleic acids. And the strong affinity of the silver ion to cytosine favors DNA oligonucleotides as ideal templates for the synthesis of fluorescent AgNCs.^{24–27} Nucleic acid-stabilized silver nanoclusters

State Key Laboratory of Chemo/Biosensing and Chemometrics, College of Chemistry and Chemical Engineering, Hunan University, Changsha, 410082, P. R. China.
E-mail: cylei@hnu.edu.cn, niezhou.hnu@gmail.com; Fax: +86-731-88821848;
Tel: +86-731-88821626

† Electronic supplementary information (ESI) available. See DOI: 10.1039/c8an00535d

(DNA/AgNCs) with various fluorescence emissions spanning the visible and near-infrared spectral regions have been prepared using different oligonucleotide sequences.^{28–30} The excellent photophysical properties and good biocompatibility turn the DNA/AgNCs to attractive materials for optical sensing and biological imaging applications. For instance, DNA/AgNCs have been applied as fluorescent probes for the detection of metal ions,^{31,32} bioactive molecules³³ and nucleic acids,^{34,35} for probing enzyme activities and screening inhibitors,^{36,37} and even for cell imaging.^{38,39} By a rational design of the chimeric oligonucleotide template, most of the DNA/AgNC probes realized switch-on fluorescence assay with a high signal-to-background ratio.⁴⁰ Such a sensing strategy is especially helpful for *in situ* cell apoptosis assay, because extra washing and separation steps can be avoided.

In eukaryotes, most nuclear-encoded messenger RNAs (mRNAs) have a sequence of the polyadenylic acid (poly-A) tail at their 3'-termini.^{41,42} Inspired by this natural phenomenon, we herein added a poly-dA tail to the apoptotic DNA fragments using the TdT-mediated template-independent DNA polymerization.^{15,43,44} Then, a novel DNA/AgNC probe for *in situ* cell apoptosis assay and imaging was developed based on the TdT-mediated polymerization and toehold strand displacement reaction. The proposed cell apoptosis assay involves (1) a non-fluorescent DNA/AgNC probe composed of DNA-stabilized AgNCs and BHQ-labeled DNA, (2) TdT-mediated elongation of the poly-dA chain using the fragmented DNA in apoptotic cells as primers, and (3) fluorescence recovery of DNA/AgNCs triggered by the toehold strand displacement between the elongated poly-dA chain and DNA/AgNC probe. Owing to the formation of long poly-dA chains, numerous AgNCs can be lighted up at each DNA fragment, thereby dramatically amplifying the fluorescence signal and consequently greatly improving the detection sensitivity. Benefiting from the ultra-low background fluorescence of the DNA/AgNC probe and switch-on signal model, *in situ* assay of apoptosis in HepG2 cells without multiple washing steps was achieved using the proposed approach. The DNA/AgNC probe not only provides a smart molecular imaging for cell apoptosis, but also holds considerable potential for basic research of apoptosis and drug evaluation for antitumor therapy.

Experimental

Materials

Silver nitrate (AgNO₃) and sodium borohydride (NaBH₄) were purchased from Sinopharm Chemical Reagent Company, Ltd (Shanghai, China). Terminal deoxynucleotidyl transferase (TdT) was purchased from Fermentas Inc. (Vilnius, Lithuania). Deoxyadenosine triphosphate (dATP), deoxythymidine triphosphate (dTTP), and SYBR Green II were obtained from Sangon (Shanghai, China). Staurosporine (STS) was purchased from Selleck Chemicals. DMEM cell culture medium was purchased from Thermo Scientific Gibco (Massachusetts, USA). RNA-simple total RNA and TIANamp genomic DNA kits were pur-

chased from TIANGEN (Beijing, China). All oligonucleotides were HPLC-purified and freeze-dried by Sangon (Shanghai, China), and the detailed sequences are shown in Table S1.† The oligonucleotides were dissolved in ultrapure water to obtain stock solutions of 100 μM. Unless otherwise noted, all the chemicals were used as received without further purification. Ultrapure water (18.2 MΩ cm) was obtained from a Millipore (Milli-Q) system and used for all experiments.

Cell culture

Liver hepatocellular cells (HepG2) were purchased from the Cell Bank of Central Laboratory at Xiangya Hospital (Changsha, China). HepG2 cells were cultured in DMEM medium supplemented with 10% heat-inactivated fetal bovine serum and 1% antibiotics (100 U mL⁻¹ streptomycin–penicillin) at 37 °C in a humidified incubator containing 5% CO₂. The number of cells were counted using a Bio-rad TC10 automated cell counter.

Synthesis and characterization of fluorescent DNA/AgNCs

In a typical experiment, 10 μL of 100 μM solution of AgNO₃ was added into 10 μL of 10 μM solutions of oligonucleotides in 10 mM phosphate buffer (10 mM Na₂HPO₄–NaH₂PO₄, pH 7.0), followed by vigorous shaking of the solution for 30 s. After 15 min, 10 μL of 100 μM NaBH₄ was added into the mixture, followed by vigorous shaking of the mixture for 30 s. The solution was kept in the dark at room temperature for 12 h.

Fluorescence emission and excitation spectra were recorded on a QuantaMaster TM4 fluorescence spectrophotometer (PTI, Canada). Transmission electron microscopy (TEM) measurements were performed on a JEM-2100F high-resolution transmission electron microscope (JEOL Ltd, Japan) with an accelerating voltage of 200 kV. Similar to the previously reported literature,⁴⁵ the synthesized DNA/AgNCs were centrifuged using a centrifugal filter unit (Amicon Ultra-0.5 mL with MWCO of 50 K, Millipore) at 5000 rpm for 30 min prior to TEM imaging. A drop of the obtained DNA/AgNC solution was carefully placed on a carbon-coated copper grid and then dried under ambient conditions for TEM characterization.

Enzymatic polymerization assay

The typical TdT-mediated polymerization experiment was performed in 10 μL of TdT buffer (1×, 0.2 M potassium cacodylate, 25 mM Tris, 0.01% (v/v) Triton X-100, 1 mM CoCl₂, pH 7.2) containing ssDNA oligo, 1 mM dATP and 4 U TdT. The mixture was incubated at 37 °C for 2 h, and the reaction was terminated by heating the solution at 70 °C for 10 min, according to the instructions supplied by the enzyme supplier.

For the analysis of the TdT polymerization products, samples were loaded into a denaturing 8% PAGE and the electrophoresis was carried out in 1× Tris-borate-EDTA (TBE) buffer (90 mM Tris, 90 mM boric acid, and 10 mM EDTA, 7 M urea, pH 8.0) for 3 h (110 V, constant voltage). The gels were scanned using a ChemiDoc™ MP System (Bio-Rad) after staining with SYBR Green II for 30 min.

Detection of the random primer

To detect different concentrations of the random primer, the polymerization experiments were conducted under the same conditions as those of the above-mentioned process except using different concentrations of the primer. The analyses were performed in a reaction volume of 100 μL including 10 mM phosphate buffer, 10 mM HEPES buffer, and 200 mM NaNO_3 (pH 7.0). The sensing modules DNA/AgNCs and S2 were incubated for 30 min and then subjected to the target poly-dA DNA chain for different time intervals, at fixed concentrations of the poly-dA DNA chain, or at a fixed time interval (24 min) for variable concentrations of the target. The final concentration of the DNA/AgNC probe was 500 nM.

In vitro detection of DSBs

For TdT-mediated polymerization initiated from DSBs, genomic DNA (gDNA) was purified from HepG2 cells according to the manufacturer's protocol of the TiANamp genomic DNA kit. Then the purified gDNA was incubated with DNase I (0.25 U) in reaction buffer at 37 $^\circ\text{C}$ for 10 min with a total volume of 10 μL , and the reaction was stopped by heating the solution at 80 $^\circ\text{C}$ for 20 min. Then TdT (5 μL , 4 U, in 2 \times reaction buffer) was added to the resulting solution (5 μL) containing DNase I-digested gDNA to initiate the polymerization. The reaction solution was incubated at 37 $^\circ\text{C}$ for 2 h and the reaction was terminated by heating the solution at 70 $^\circ\text{C}$ for 10 min. The analytical experiments were conducted in the same way as the above-mentioned analysis process.

In situ imaging and detection of cell apoptosis

HepG2 cells (2×10^4 cells per each dish) were cultured in confocal dishes with a 14 mm bottom well in DMEM medium at 37 $^\circ\text{C}$. After 80% confluence, the coverslips were washed twice with PBS buffer and the medium was replaced with fresh DMEM medium containing STS (1 μM). After incubation at 37 $^\circ\text{C}$ for different times, the cells were washed twice with PBS buffer. Next, the cells were fixed in 4% paraformaldehyde at room temperature for 20 min, rinsed three times with PBS buffer, permeabilized with 1% Triton X-100 in PBS for 5 min, and then rinsed three times again with PBS buffer at room temperature. Then, 50 μL of TdT buffer, 60 U of TdT, and 1 mM dATP were added to cell samples. And the cell samples were incubated at 37 $^\circ\text{C}$ for 1 h in a humidified chamber. Thereafter, all the nuclei were stained with DAPI for 10 min, and then rinsed three times with PBS buffer. Next, the cell samples were reacted with 1.5 μM DNA/AgNC probes (10 mM phosphate buffer, 10 mM HEPES buffer, and 200 mM NaNO_3 , pH 7.0) for 30 min. Subsequently, stained cells were directly visualized on a confocal laser scanning microscope (CLSM, C1-Si, Nikon, Japan). DAPI was excited with a 405 nm laser diode and the emission was collected from 420 to 480 nm. The fluorescence of the released DNA/AgNCs was collected from 675 to 725 nm on the microscope with an excitation wavelength of 640 nm. The images were acquired and processed using Image J (NIH). The number of DNA/AgNC-positive cells at the Cy5

channel and total cell number at the DAPI channel were quantified and averaged from five randomly chosen microscopic fields (magnification $\times 200$, 40–100 cells from each microscopic field). The apoptosis rates were determined as the percentage of DNA/AgNC-positive cells of total cells in each condition. Apoptosis rates at various induced times were plotted against induced time. Values are represented as means \pm standard deviation (SD) of three independent experiments.

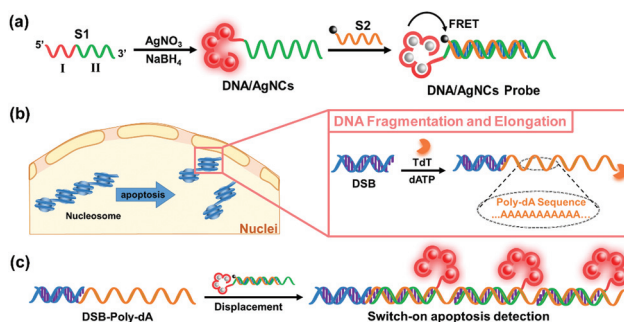
Results and discussion

Principle of the DNA/AgNC probe for cell apoptosis assay

The principle of the DNA/AgNC probe for cell apoptosis assay is detailed in Scheme 1. To fabricate a switch-on fluorometric DNA/AgNC probe, a single strand DNA S1 that contains two domains I and II is applied. Cytosine-rich domain I exhibits strong affinity toward the Ag^+ ion, and fluorescent nucleic acid-stabilized AgNCs can be readily prepared by the reduction of Ag^+ to Ag^0 . As domain II is partially hybridized with BHQ-labeled DNA S2, the quencher resides in proximity to the AgNCs, which results in efficient quenching of the fluorescence of DNA/AgNCs by fluorescence resonance energy transfer (FRET). In the nucleus of apoptotic cells, TdT catalyzes the addition of poly-dA to the 3'-OH ends of the DSBs, using DSBs and dATP as the primer and substrate, respectively. Then, the elongated poly-dA chains hybridize with the 3' poly-T overhangs of the DNA/AgNC probe, and initiate the toehold strand displacement, thereby resulting in the quencher-labeled S2 moving from the DNA/AgNC probe and subsequent recovery of the fluorescence of DNA/AgNCs. Therefore, such a signal-on design provides a quantitative fluorescence measurement of cell apoptosis without extra washing.

Fabrication of the fluorescent DNA/AgNC probe

Following the design, a ssDNA S1 containing a 24-nt nucleation sequence for Ag^+ (domain I) and a 28-nt poly-T sequence (domain II) was used as the template to synthesize the AgNCs according to a reported method.^{32,46} As depicted in Fig. 1a, the as-prepared DNA/AgNCs emitted red fluorescence with the



Scheme 1 Schematic illustration of *in situ* cell apoptosis detection. (a) The synthesis of the DNA/AgNC probe. (b) DNA fragmentation and TdT-mediated elongation assay in the apoptotic cell. (c) *In situ* cell apoptosis detection utilizing the DNA/AgNC probe.

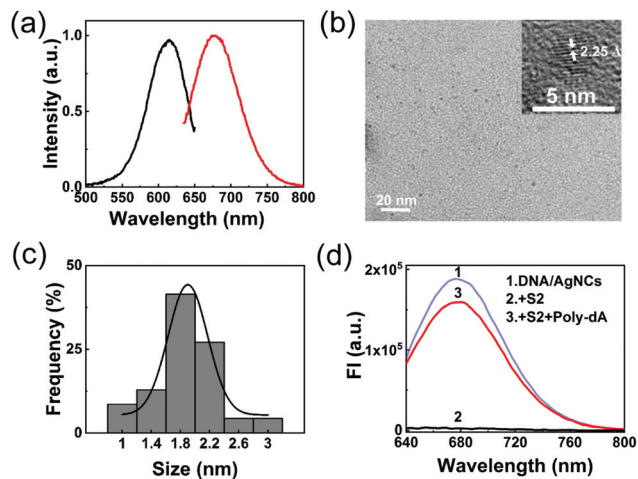


Fig. 1 Characterization of the as-prepared DNA/AgNCs. (a) Excitation and emission spectra, (b) TEM images and lattice fringes (inset image), and (c) size distribution of DNA/AgNCs. (d) Fluorescence spectra of DNA/AgNCs, and the DNA/AgNC probe in the absence and presence of the poly-dA chain. The concentrations of DNA/AgNCs, S2 and poly-dA were 500 nM, 500 nM, and 50 nM, respectively.

maximum excitation and emission wavelengths of 615 nm and 675 nm, respectively. According to the transmission electron microscopy (TEM, Fig. 1b and c) image, the DNA/AgNCs were monodispersed with an average diameter of 1.92 ± 0.49 nm. In addition, the high-resolution transmission electron microscopy image (HR-TEM, Fig. 1b inset) shows that the lattice fringes of DNA/AgNCs are 2.25 Å, which is consistent with the interplanar spacing of the (111) crystal plane of face-centered cubic Ag.⁴⁴ Moreover, the DNA/AgNCs maintain 93% of the initial fluorescence after ten days of storage in the dark at 4 °C, indicating the relatively good stability of the DNA/AgNCs.

Then, the DNA/AgNCs were incubated with an equal amount of BHQ-labeled DNA S2 for the fabrication of the DNA/AgNC probe. As shown in Fig. S2,† there is a good overlap between the absorption spectra of the quencher and the fluorescence spectra of the DNA/AgNCs. Owing to the close proximity between DNA/AgNCs and BHQ induced by DNA hybridization, the fluorescence of DNA/AgNCs was efficiently quenched with a quenching rate of up to 98.5% by FRET (Fig. 1d). Such a high quenching efficacy endows the proposed probe with the advantage of an ultra-low background signal.

A random primer model

Firstly, a random ssDNA sequence was chosen as the model primer to simulate the DSBs in apoptotic cells for *in vitro* experiments. Using dATP as the substrate, the poly-dA products of TdT-mediated elongation were analyzed by denaturing polyacrylamide gel electrophoresis (PAGE). As shown in Fig. 2a, the length of the elongated poly-dA chain increased with an increase of elongation time, and it could reach up to approximately 400 bases at an elongation time of 120 min.

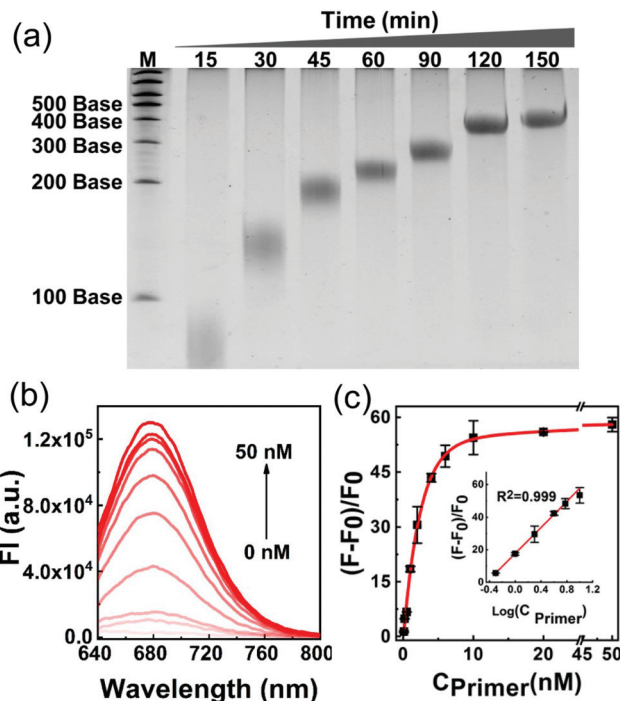


Fig. 2 (a) Analysis of the elongated poly-dA products of the random primer (500 nM) at different elongation times by denaturing PAGE (8%). (b) Fluorescence spectra of the DNA/AgNC probe upon the addition of poly-dA chains elongated at different concentrations of the primer. (c) Fluorescence responses of the DNA/AgNC probe to poly-dA chains elongated at different concentrations of the primer. F_0 and F are the fluorescence intensity of the DNA/AgNC probe at 675 nm in the absence and presence of poly-dA chains, respectively. The inset shows the linear responses to the primer in the low concentration range. The concentrations of TdT and dATP are 40 U mL⁻¹ and 100 μM, respectively.

Then, the elongated poly-dA DNA chains were incubated with the DNA/AgNC probe. The efficient toehold strand displacement between the poly-dA chain and S1 caused a significant restoring of the fluorescence of DNA/AgNCs, about 80% of their initial fluorescence intensity, providing a high signal-to-background ratio of 58. To verify whether the fluorescence response is due to the presence of poly-dA chains, dTTP, dCTP, dGTP, and dNTPs were used as substrates of TdT under the same conditions to generate poly-dT, poly-dC, poly-dG and random DNA sequences, respectively. Mixing these elongation products with the DNA/AgNC probe, negligible fluorescence enhancements were observed (Fig. S3†). These results indicate that the proposed probe is highly sensitive and selective toward poly-dA chains.

Then the dynamics of the fluorescence response of the DNA/AgNC probe toward the poly-dA chain was investigated by monitoring the fluorescence intensity change *versus* incubation time. The fluorescence of DNA/AgNCs increased quickly in the first 4 min (increased ~39-fold), and then gradually increased with an increase of incubation time and tented to a saturation point at 24 min (Fig. S4†). Next, the sensitivity of the DNA/AgNC probe was evaluated by measuring the fluo-

rescence response toward different concentrations of the random primer. When the concentration of the random primer increased from 0.2 to 50 nM, the fluorescence intensity of DNA/AgNCs continually increased (Fig. 2b). The plot of the fluorescence response *versus* the concentration of the random primer is shown in Fig. 2c with a plateau point at 10 nM of the random primer. The log concentration of the primer ($\log c_{\text{primer}}$) and fluorescence response ($(F - F_0)/F_0$) were used for the data fit, and a linear equation $y = 40.0x - 17.7$ ($R^2 = 0.999$) from 0.5 to 10 nM was obtained with a limit of detection of 0.2 nM (inset of Fig. 2c). Taken together, the quick and dramatic fluorescence response of the DNA/AgNC probe might provide a sensitive fluorometric assay for the quantitative detection of DSBs in apoptotic cells.

In vitro detection of DSBs

To test the feasibility of the DNA/AgNC probe in detecting DSBs, genomic DNA (gDNA) of HepG2 cells was digested by DNase I to generate short DNA fragments,^{47,48} followed by TdT-mediated polymerization to generate the poly-dA chain. Upon addition of the DNA/AgNC probe, the fluorescence intensity gradually increased as the concentration of gDNA increased from 0.13 to 13 ng (Fig. 3a), which corresponds to 20–2000 cells. A linear range from 0.13 to 6.5 ng was obtained with the lowest detection amount of 0.13 ng (inset of Fig. 3a). No obvious fluorescence responses were observed when the gDNA was treated with TdT or DNase I alone (Fig. 3b).

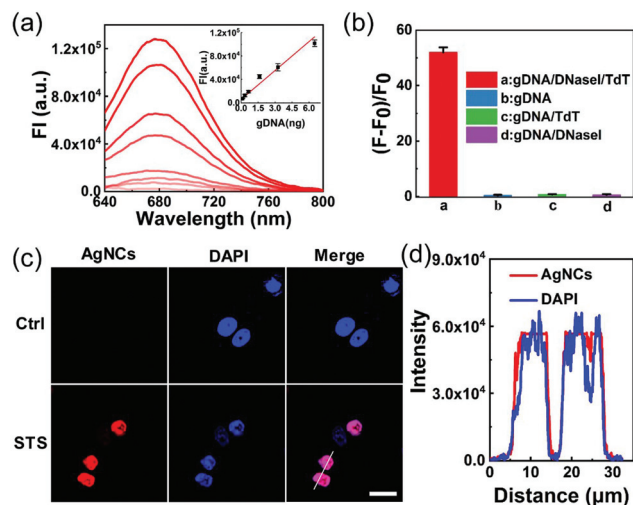


Fig. 3 (a) Fluorescence spectra of the DNA/AgNC probe in the presence of poly-dA chains elongated at different amounts (0.13, 0.325, 0.65, 1.625, 3.25, 6.5 and 13 ng) of DNase I-digested gDNA. The inset shows the linear response range to DNase I-digested gDNA. (b) Fluorescence response of the DNA/AgNC probe under different treatments. (c) Apoptosis detection in cultured cells using the DNA/AgNC probe. Nuclei were counterstained with DAPI; the scale bar is 25 μm . (d) Colocalization analysis of blue and red fluorescence channels of left images.

In situ imaging and detection of cell apoptosis

Prior to cellular application, the potential effects of various components in the complex cellular environment including amino acid, proteins and nucleic acids on the stability of the DNA/AgNCs were evaluated. As shown in Fig. S5a,[†] the existence of several amino acids did not induce any significant influence on the fluorescence of DNA/AgNCs. Similarly, the presence of other cellular macromolecules including bovine serum albumin (BSA), cytochrome c (Cyt c), ascorbic acid, adenosine and thrombin also caused negligible effects on the fluorescence of DNA/AgNCs. Moreover, gDNA, total RNA and apoptotic cell lysate have little influence on the stability of the DNA/AgNCs (Fig. S5b[†]). The above results confirmed that DNA/AgNCs can maintain the material-stability in a complex cellular environment, suggesting its potential in analysis of apoptotic DSBs at the cellular level.

The validity of the DNA/AgNC-based assay for apoptosis detection at the cellular level was further evaluated. HepG2 cells were treated with a typical apoptosis chemo-inducer (staurosporine, STS) that activates the caspase 3 apoptotic pathway,⁴⁹ and the induced apoptotic cells were used as a model. The apoptotic HepG2 cells were fixed in 4% paraformaldehyde, and permeabilized with Triton X-100.⁵⁰ After these processes, the cell and nucleus became permeable to the TdT, dATP and DNA/AgNC probe. Then the fixed cells were incubated with TdT and dATP to generate poly-dA DNA chains. Finally, the DNA/AgNC probe was added and the fixed cells were directly imaged by using a confocal laser scanning microscope (CLSM) without extra washing steps. The apoptotic cells showed a strong red fluorescence signal at the Cy5 channel (Fig. 3c), while no fluorescence was observed in the control cells. These results clearly demonstrated that our approach can effectively distinguish and identify a single apoptotic cell.

To confirm that the activated fluorescent signal came from the DSBs of cleaved chromatin during cell apoptosis, all cells were cotreated with 4',6-diamidino-2-phenylindole (DAPI) for nuclei staining. A perfect colocalization of DNA/AgNCs and DAPI was observed (Fig. 3d) and further quantified using Manders' overlap coefficient. A high overlap coefficient of 0.97 was obtained, indicating that the *de novo* poly-dA chains are formed within the nuclei of apoptotic cells. Whereas, when the apoptotic cells were incubated with only dATP pool or TdT, no obvious fluorescence signal was observed (Fig. S6,[†] parts 2 and 3), indicating that the fluorescence signal derives from the enzymatic polymerization and cellular components had little interference with the fluorescence signal. To test whether the signals came from the ssDNA synthesized by TdT, the apoptotic cells were incubated with TdT and dATP, and then treated with S1 nuclease, which cleaves ssDNA into oligo- or mononucleotides.⁵¹ Upon the addition of the DNA/AgNC probe, no detectable fluorescence was observed (Fig. S6,[†] part 4), suggesting that the signal was from the newly synthesized ssDNA. To verify the fluorescence signal is specific for poly-dA chains, dATP was replaced by dTTP to generate poly-dT DNA chains by TdT. On this occasion, the fluorescence signal was

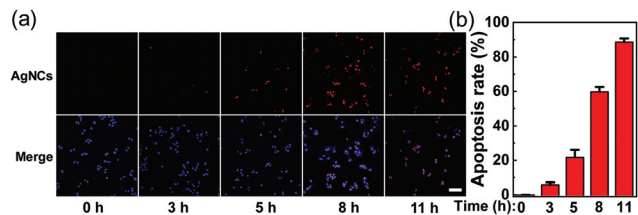


Fig. 4 (a) Apoptosis detection in cultured cells using the DNA/AgNC-based assay. HepG2 Cells were incubated with STS ($1 \mu\text{M}$) for different time intervals to induce apoptosis. Representative CLSM images are shown, and the scale bar is $100 \mu\text{m}$. (b) The quantified apoptotic ratios at different incubation times.

completely abolished (Fig. S6,† part 5), implying that the signal is specifically from the poly-dA DNA chain. Besides, the addition of GSH (3 mM), an efficient quencher of DNA/AgNCs,⁵² remarkably eliminated the fluorescence signals (Fig. S6,† part 6), which demonstrates that the fluorescence signal comes from the DNA/AgNCs.

Next, the DNA/AgNC-based apoptotic assay was performed without or with washing steps, and bright red fluorescence of the apoptotic cells could be observed with high signal-to-background ratios (S/B, 43.5 and 45.5, respectively.) under both conditions (Fig. S7a and S7b†), providing a wash-free method for cell apoptosis assay. However, a previous study has demonstrated that traditional TUNEL assay requires multiple washing and incubating steps to eliminate the strong background of the labeled nucleotides (*e.g.*, FITC-dUTP).¹⁵ Then, the feasibility of the DNA/AgNC-based assay in quantitative analysis of apoptotic cell fraction in cultured cell samples was evaluated. HepG2 cells were treated with STS for different times and subjected to TdT-mediated elongation and the DNA/AgNC probe. As shown in Fig. 4a, red fluorescence of DNA/AgNCs could be clearly seen in cells that are exposed to STS for 3 h, and the number of cells with bright fluorescence gradually mounts up with an increase of incubation time. According to the cell number ratio of red fluorescence-positive cells to the total cells, the apoptotic ratios in the group of the cells treated with STS for 3 h, 5 h, 8 h and 11 h were counted to 5.8%, 21.7%, 59.7% and 88.5%, respectively (Fig. 4b). We further applied an Annexin V-FITC/PI apoptosis analysis kit for quantitative apoptosis analysis. Similarly, the rate of late apoptosis in the group of cells treated with $1 \mu\text{M}$ STS for 3 h and 8 h was estimated as 4.5% and 57.1% (Fig. S8†), respectively, consistent well with the corresponding data of the DNA/AgNC-based apoptotic assay. This result implies the potential application of the DNA/AgNC-based assay in quantitative analysis of cell apoptosis.

Conclusions

In this work, we have developed a novel DNA/AgNC probe for *in situ* apoptotic cell detection and imaging based on the TdT-mediated polymerization and toehold strand displacement reaction. Benefiting from the ultra-low background fluo-

rescence of the probe and high efficiency of the strand displacement, sensitive and quantitative detection of apoptosis was achieved at the cellular level using the DNA/AgNC-based assay. Compared with conventional TUNEL assays that require tedious washing steps, the switch-on signal pattern endows the proposed assay with facile and wash-free procedures. Considering the sequence-controlled fluorescence properties of metallic NCs and the availability of different nucleic acid-stabilized luminescent metal nanostructures, the proposed sensing strategy may be expanded for several advanced bio-imaging applications, such as *in situ* biomolecule detection, multiple target imaging and even imaging in living cells.

Conflicts of interest

There are no conflicts to declare.

Acknowledgements

This work was financially supported by the National Natural Science Foundation of China (No. 21505120, 21575038 and 21235002) and the Foundation for Innovative Research Groups of NSFC (Grant 21521063), and the Fundamental Research Funds for the Central Universities.

Notes and references

- 1 Y. Fuchs and H. Steller, *Cell*, 2011, **147**, 742–758.
- 2 S. M. Hurlley, *Science*, 2016, **352**, 48–50.
- 3 M. O. Hengartner, *Nature*, 2000, **407**, 770–776.
- 4 H. Okada and T. W. Mak, *Nat. Rev. Cancer*, 2004, **4**, 592–603.
- 5 T. T. Chen, X. Tian, C. L. Liu, J. Ge, X. Chu and Y. Li, *J. Am. Chem. Soc.*, 2015, **137**, 982–989.
- 6 Y. Li, P. Li, R. Zhu, C. Luo, H. Li, S. Hu, Z. Nie, Y. Huang and S. Yao, *Anal. Chem.*, 2016, **88**, 11184–11192.
- 7 Y. Pan, M. Guo, Z. Nie, Y. Huang, Y. Peng, A. Liu, M. Qing and S. Yao, *Chem. Commun.*, 2012, **48**, 997–999.
- 8 H. Wang, Q. Zhang, X. Chu, T. Chen, J. Ge and R. Yu, *Angew. Chem., Int. Ed.*, 2011, **50**, 7065–7069.
- 9 S. Elmore, *Toxicol. Pathol.*, 2007, **35**, 495–516.
- 10 S. Nagata, *Exp. Cell Res.*, 2000, **256**, 12–18.
- 11 H. Shi, X. He, K. Wang, Y. Yuan, K. Deng, J. Chen and W. Tan, *Nanomedicine*, 2007, **3**, 266–272.
- 12 O. Krysko, R. L. De and M. Cornelissen, *Apoptosis*, 2004, **9**, 495.
- 13 S. Huerta, E. J. Goulet, S. Huerta-Yepe and E. H. Livingston, *J. Surg. Res.*, 2007, **139**, 143–156.
- 14 Z. Darzynkiewicz, D. Galkowski and H. Zhao, *Methods*, 2008, **44**, 250–254.
- 15 Z. Liu, X. Luo, Z. Li, Y. Huang, Z. Nie, H. H. Wang and S. Yao, *Anal. Chem.*, 2017, **89**, 1892–1899.
- 16 G. D. Sloop, J. C. Roa, A. G. Delgado, J. T. Balart and J. M. Hill, *Arch. Pathol. Lab. Med.*, 1999, **123**, 529.

- 17 J. Li, J.-J. Zhu and K. Xu, *TrAC, Trends Anal. Chem.*, 2014, **58**, 90–98.
- 18 Y. Tao, M. Li, J. Ren and X. Qu, *Chem. Soc. Rev.*, 2015, **44**, 8636–8663.
- 19 X. R. Song, N. Goswami, H. H. Yang and J. Xie, *Analyst*, 2016, **141**, 3126–3140.
- 20 L. Zhang and E. Wang, *Nano Today*, 2014, **9**, 132–157.
- 21 Y. Wang, Y. Cui, Y. Zhao, R. Liu, Z. Sun, W. Li and X. Gao, *Chem. Commun.*, 2012, **48**, 871–873.
- 22 J. Xie, Y. Zheng and J. Y. Ying, *J. Am. Chem. Soc.*, 2009, **131**, 888.
- 23 P. Zhao, K. He, Y. Han, Z. Zhang, M. Yu, H. Wang, Y. Huang, Z. Nie and S. Yao, *Anal. Chem.*, 2015, **87**, 9998–10005.
- 24 J. T. Petty, J. Zheng, N. V. Hud and R. M. Dickson, *J. Am. Chem. Soc.*, 2004, **126**, 5207–5212.
- 25 C. M. Ritchie, K. R. Johnsen, J. R. Kiser, Y. Antoku, R. M. Dickson and J. T. Petty, *J. Phys. Chem. C*, 2007, **111**, 175.
- 26 J. Sharma, R. C. Rocha, M. L. Phipps, H. C. Yeh, K. A. Balatsky, D. M. Vu, A. P. Shreve, J. H. Werner and J. S. Martinez, *Nanoscale*, 2012, **4**, 4107–4110.
- 27 T. Vosch, Y. Antoku, J. C. Hsiang, C. I. Richards, J. I. Gonzalez and R. M. Dickson, *Proc. Natl. Acad. Sci. U. S. A.*, 2007, **104**, 12616–12621.
- 28 I. Diez and R. H. Ras, *Nanoscale*, 2011, **3**, 1963–1970.
- 29 C. I. Richards, S. Choi, J. C. Hsiang, Y. Antoku, T. Vosch, A. Bongiorno, Y. L. Tzeng and R. M. Dickson, *J. Am. Chem. Soc.*, 2008, **130**, 5038.
- 30 Z. Yuan, Y. C. Chen, H. W. Li and H. T. Chang, *Chem. Commun.*, 2014, **50**, 9800–9815.
- 31 L. Gong, H. Kuai, S. Ren, X. H. Zhao, S. Y. Huan, X. B. Zhang and W. Tan, *Chem. Commun.*, 2015, **51**, 12095–12098.
- 32 G. Y. Lan, C. C. Huang and H. T. Chang, *Chem. Commun.*, 2010, **46**, 1257–1259.
- 33 M. Zhang, S. M. Guo, Y. R. Li, P. Zuo and B. C. Ye, *Chem. Commun.*, 2012, **48**, 5488–5490.
- 34 X. Liu, F. Wang, R. Aizen, O. Yehezkeli and I. Willner, *J. Am. Chem. Soc.*, 2013, **135**, 11832–11839.
- 35 P. Shah, S. W. Choi, H. J. Kim, S. K. Cho, Y. J. Bhang, M. Y. Ryu, P. W. Thulstrup, M. J. Bjerrum and S. W. Yang, *Nucleic Acids Res.*, 2016, **44**, e57.
- 36 C. Y. Lee, K. S. Park, Y. K. Jung and H. G. Park, *Biosens. Bioelectron.*, 2017, **93**, 293–297.
- 37 X. Liu, F. Wang, A. Niazov-Elkan, W. Guo and I. Willner, *Nano Lett.*, 2013, **13**, 309–314.
- 38 G. Liu, J. Li, D. Q. Feng, J. J. Zhu and W. Wang, *Anal. Chem.*, 2017, **89**, 1002–1008.
- 39 J. Yin, X. He, K. Wang, F. Xu, J. Shangguan, D. He and H. Shi, *Anal. Chem.*, 2013, **85**, 12011–12019.
- 40 J. T. Del Bonis-O'Donnell, D. K. Fygenson and S. Pennathur, *Analyst*, 2015, **140**, 1609–1615.
- 41 B. Tian, J. Hu, H. Zhang and C. S. Lutz, *Nucleic Acids Res.*, 2005, **33**, 201–212.
- 42 N. Viphakone, F. Voisinet-Hakil and L. Minvielle-Sebastia, *Nucleic Acids Res.*, 2008, **36**, 2418–2433.
- 43 Z. Liu, W. Li, Z. Nie, F. Peng, Y. Huang and S. Yao, *Chem. Commun.*, 2014, **50**, 6875–6878.
- 44 Y. Yuan, W. Li, Z. Liu, Z. Nie, Y. Huang and S. Yao, *Biosens. Bioelectron.*, 2014, **61**, 321–327.
- 45 L. Zhang, J. Zhu, S. Guo, T. Li, J. Li and E. Wang, *J. Am. Chem. Soc.*, 2013, **135**, 2403–2406.
- 46 G.-Y. Lan, W.-Y. Chen and H.-T. Chang, *RSC Adv.*, 2011, **1**, 802–807.
- 47 M. Oliveri, A. Daga, C. Cantoni, C. Lunardi, R. Millo and A. Puccetti, *Eur. J. Immunol.*, 2001, **31**, 743–751.
- 48 V. J. Yuste, I. Sanchez-Lopez, C. Sole, R. S. Moubarak, J. R. Bayascas, X. Dolcet, M. Encinas, S. A. Susin and J. X. Comella, *J. Biol. Chem.*, 2005, **280**, 35670–35683.
- 49 H. J. Chae, J. S. Kang, J. O. Byun, K. S. Han, D. U. Kim, S. M. Oh, H. M. Kim, S. W. Chae and H. R. Kim, *Pharmacol. Res.*, 2000, **42**, 373–381.
- 50 M. A. Melan, in *Immunocytochemical Methods and Protocols*, Springer, 1994, pp. 55–66.
- 51 X. Yang, F. Pu, J. Ren and X. Qu, *Chem. Commun.*, 2011, **47**, 8133–8135.
- 52 B. Han and E. Wang, *Biosens. Bioelectron.*, 2011, **26**, 2585–2589.